Biofilm 2 (2020) 100039

Contents lists available at ScienceDirect

Biofilm

journal homepage: www.elsevier.com/locate/bioflm

Nontypeable *Haemophilus influenzae* newly released (NRel) from biofilms by antibody-mediated dispersal *versus* antibody-mediated disruption are phenotypically distinct

Elaine M. Mokrzan [a,1], Christian P. Ahearn [a,1,2], John R. Buzzo [a], Laura A. Novotny [a,1], Yan Zhang [b,c], Steven D. Goodman [a,d], Lauren O. Bakaletz [a,d,*]

[a] Center for Microbial Pathogenesis, Abigail Wexner Research Institute at Nationwide Children's Hospital, Columbus, OH, USA
[b] Department of Biomedical Informatics, The Ohio State University College of Medicine, Columbus, OH, USA
[c] The Ohio State University Comprehensive Cancer Center (OSUCCC – James), Columbus, OH, USA
[d] Department of Pediatrics, The Ohio State University College of Medicine, Columbus, OH, USA

ARTICLE INFO

Keywords:
Chronic infection
Disruption
Dispersal
Antibiotic
Proteomics
Quorum sensing

ABSTRACT

Biofilms contribute significantly to the chronicity and recurrence of bacterial diseases due to the fact that biofilm-resident bacteria are highly recalcitrant to killing by host immune effectors and antibiotics. Thus, antibody-mediated release of bacteria from biofilm residence into the surrounding milieu supports a powerful strategy to resolve otherwise difficult-to-treat biofilm-associated diseases. In our prior work, we revealed that antibodies directed against two unique determinants of nontypeable *Haemophilus influenzae* (NTHI) [e.g. the Type IV pilus (T4P) or a bacterial DNABII DNA-binding protein, a species-independent target that provides structural integrity to bacterial biofilms] release biofilm-resident bacteria via discrete mechanisms. Herein, we now show that the phenotype of the resultant newly released (or NRel) NTHI is dependent upon the specific mechanism of release. We used flow cytometry, proteomic profiles, and targeted transcriptomics to demonstrate that the two NRel populations were significantly different not only from planktonically grown NTHI, but importantly, from each other despite genetic identity. Moreover, each NRel population had a distinct, significantly increased susceptibility to killing by either a sulfonamide or β-lactam antibiotic compared to planktonic NTHI, an observation consistent with their individual proteomes and further supported by relative differences in targeted gene expression. The distinct phenotypes of NTHI released from biofilms by antibodies directed against specific epitopes of T4P or DNABII binding proteins provide new opportunities to develop targeted therapeutic strategies for biofilm eradication and disease resolution.

Introduction

The Centers for Disease Control and Prevention and the National Institutes of Health estimate that biofilms contribute to the pathogenesis of ~80% of all bacterial infections [1]. Biofilm-associated diseases such as otitis media (OM), cystic fibrosis, chronic obstructive pulmonary disease, chronic rhinosinusitis, chronic wound infections, periodontitis, cystitis and infections of medical implants and indwelling catheters, among many others, are typically chronic and/or recurrent due to the presence of bacteria within biofilms that are highly resistant to killing by host immune effectors and antibiotics [2,3]. Our laboratory has primarily focused on diseases of the upper and lower respiratory tracts caused by nontypeable *Haemophilus influenzae* (NTHI) wherein a biofilm contributes significantly to each disease course [4–6]. An example of one such disease wherein NTHI is the predominant pathogen is OM [7–11], the most common bacterial disease in children [12,13]. The role of biofilms in OM pathogenesis, chronicity and recurrence is widely accepted. Nonetheless, like most NTHI-induced diseases, OM is still commonly

* Corresponding author. Abigail Wexner Research Institute at Nationwide Children's Hospital, 700 Children's Drive, W591, Columbus, OH, 43205, USA.
E-mail addresses: elaine.mokrzan@nationwidechildrens.org (E.M. Mokrzan), cpahearn@buffalo.edu (C.P. Ahearn), john.buzzo@nationwidechildrens.org (J.R. Buzzo), laura.novotny@nationwidechildrens.org (L.A. Novotny), zhangyan.thu2001@gmail.com (Y. Zhang), steven.goodman@nationwidechildrens.org (S.D. Goodman), Lauren.Bakaletz@nationwidechildrens.org (L.O. Bakaletz).
[1] These individuals contributed equally.
[2] Department of Oral Biology, University at Buffalo, The State University of New York, Buffalo, NY.

https://doi.org/10.1016/j.bioflm.2020.100039
Received 7 August 2020; Received in revised form 2 November 2020; Accepted 12 November 2020
Available online 18 November 2020

treated with broad-spectrum oral antibiotics, which do not reach sufficient levels in the middle ear (or other sites) to eradicate biofilms or even the planktonically growing bacteria within this anatomical niche [14]. Although their use is sometimes indicated or necessary, broad-spectrum antibiotics can also cause collateral damage in the form of skin rashes, diarrhea and life-long disruption of the gut microbiome, with accompanied immunological and/or developmental consequences [15–17]. Moreover, the all too common indiscriminate and often ineffective use of antibiotics contributes greatly to the globally burgeoning problem of development of multiple antibiotic-resistant bacteria [18–20].

Delivery of vaccines is the most cost-effective way to manage infectious diseases as these target prevention [21], and as such, vaccine development remains a viable and truly ideal goal. However, for those children and adults with existing biofilm-associated chronic or recurrent infections, an effective therapeutic approach is greatly needed. In our long-standing efforts to develop a vaccine for diseases of the respiratory tract caused by NTHI, we focused on two unique, biofilm-associated determinants. Our first target is the NTHI T4P, a critical adhesin with multiple roles in adherence, colonization, biofilm formation, twitching motility and competence [22–28]. Antibodies against the majority subunit of NTHI T4P (PilA), and specifically a recombinant and soluble form of PilA ('rsPilA'), induce dispersal of pre-existing NTHI as well as polymicrobial biofilms *in vitro*, and also those present within the middle ear in a chinchilla model of NTHI-induced OM wherein biofilm dispersal leads to rapid disease resolution [29–34]. The mechanism for this outcome requires expression of both T4P and LuxS, the latter mediates quorum sensing in NTHI [35–37]. Armbruster et al. showed that *luxS*-induced production of the quorum-sensing molecule autoinducer 2 (AI-2) leads to increased biofilm formation *in vitro* and persistence *in vivo* in a chinchilla model of OM [35], and further revealed that NTHI takes up AI-2 from its environment via RbsB [38]. The role of *luxS*-mediated AI-2 signaling in biofilm maturation and prevention of biofilm dispersal was further demonstrated by Pang et al., who used an NTHI construct wherein *luxS* expression was inducible [39].

Our studies revealed an additional role for *luxS* quorum signaling specifically during biofilm dispersal induced by anti-rsPilA antibodies, which requires both NTHI T4P expression and *luxS*-induced production of AI-2 [33]. NTHI are released in a 'top down' process, with maximal dispersal into the supernatant within 6 h of incubation [29,33]. Armbruster et al. also showed that *Moraxella catarrhalis*, which does not express AI-2, nonetheless "eavesdrops" on the AI-2 signal produced by NTHI within a polymicrobial biofilm formed by these two species, which leads to increased *M. catarrhalis* biofilm formation [40]. Intriguingly, when we incubated a pre-formed dual-species NTHI plus *M. catarrhalis* biofilm with antibody directed against rsPilA (to target an antigen expressed exclusively by NTHI), both NTHI and *M. catarrhalis* were dispersed from the biofilm [29]. The mechanism for *M. catarrhalis* dispersal revealed another example wherein *M. catarrhalis* had eavesdropped on the AI-2 produced by NTHI in response to exposure to anti-rsPilA [29].

Our second target, Integration Host Factor (IHF), is a critical structural element of the bacterial biofilm matrix. IHF and HU (a histone-like protein) comprise the ubiquitous two-membered DNABII family of bacterial DNA-binding proteins. Genes that encode IHF and/or HU are present in the genome of every member of Eubacteria [41]. Hence, this target is not unique to NTHI but is instead species-independent due to its presence in all tested pathogen-formed biofilms to date, including each of the high priority ESKAPE pathogens (*Enterococcus faecium*, *Staphylococcus aureus*, *Klebsiella pneumoniae*, *Acinetobacter baumannii*, *Pseudomonas aeruginosa* and *Enterobacter* spp.) [42–44]. Extracellular DNA (eDNA) and associated DNABII proteins are essential to the underlying architecture and structural integrity of these biofilms [3,45–47]. Within the biofilm matrix, crossed strands of eDNA are stabilized by IHF and HU [45]. The result is a lattice-like eDNA scaffold that supports and maintains the biofilm architecture. Exposure of bacterial biofilms to antibody against DNABII proteins destabilizes the eDNA matrix and causes collapse of the biofilm structure [45]. The mechanism for this outcome is induction of an equilibrium shift wherein DNABII molecules in the milieu that surrounds the biofilm are sequestered due to formation of an antibody complex, thus DNABII proteins within the eDNA matrix are released [32,48]. The result is a sudden, complete collapse of the eDNA scaffold and release of the biofilm-resident bacteria that begins within 3 min of exposure to anti-DNABII antibodies *in vitro* [48,49]. Vaccination-induced antibodies against DNABII proteins disrupt pre-existing biofilms in a chinchilla model of NTHI-induced OM which permits clearance by host immune effectors [32,45,49]. Moreover, therapeutic treatment with anti-DNABII antibodies resolves osteolytic peri-implantitis in a rat model of pre-existing *Aggregatibacter actinomycetemcomitans* biofilms [50], and also eradicates aggregate biofilms of *P. aeruginosa* from the murine lung [32].

Despite the fact that the mechanisms and kinetics of the two targeted antisera used here are very different, the outcome of exposure of NTHI biofilms to anti-rsPilA antibodies or anti-DNABII antibodies is release of NTHI from biofilm residence into the surrounding milieu. Pioneering work from several laboratories reveals that bacteria released from a biofilm demonstrate a distinct phenotype from their biofilm-resident or planktonic counterparts [51–53]. Of note, a common characteristic of these released bacteria is sensitivity to antibiotic killing greater than that shown by even planktonically grown bacteria [29,48,54,55]. Intriguingly, whereas *P. aeruginosa* released from a biofilm by exposure to either glutamate or nitric oxide showed variable sensitivity to tobramycin and/or colistin compared to each other, both populations were more sensitive to antibiotic killing than their planktonic counterparts [54,56]. We showed that NTHI and *M. catarrhalis* released from a dual species biofilm by anti-rsPilA antibodies are significantly more sensitive to killing by either trimethoprim plus sulfamethoxazole or clarithromycin, respectively, than their agar-grown counterparts [29]. Moreover, NTHI biofilms exposed to anti-DNABII antibodies in combination with antibiotics significantly augments killing of the newly released NTHI by all three first-line antibiotics used to treat OM (e.g. ampicillin, amoxicillin-clavulanate, cefdinir) *in vitro* [48]. Further, our *in vivo* studies demonstrate that treatment with anti-DNABII antibodies in combination with the aminoglycoside antibiotic tobramycin confers an added benefit to the eradication of *P. aeruginosa* from the murine lung compared to treatment with antibodies or antibiotic alone [32].

Herein we used NTHI as a model organism to further characterize the phenotype of newly released bacteria, hereafter referred to as 'NRel'. Given the unique ways in which NTHI are released from biofilms by anti-rsPilA compared to anti-DNABII antibodies, we used comparative analysis of abundances of all expressed proteins (as determined by quantitative mass spectrometry), targeted transcriptomics, flow cytometry and susceptibility to killing by a sulfonamide or β-lactam antibiotic to investigate whether anti-rsPilA induced NRel NTHI [33] were phenotypically different than anti-DNABII induced NRel NTHI [48], despite the genetic identity of these two populations.

Material and methods

Collection and quantitation of NRel NTHI

Nontypeable *Haemophilus influenzae* strain 86-028NP is a clinical isolate recovered from the nasopharynx of a child undergoing tympanostomy tube insertion due to chronic OM [57,58] and has been maintained frozen at a low passage number. NTHI biofilms were established in brain heart infusion broth supplemented (sBHI) with 2 μg each of β-nicotinamide adenine dinucleotide (β-NAD) and heme per ml for 16 h in 8-well chambered coverglass slides as described [59]. After 16 h, biofilms were washed with 200 μl of equilibrated (37 °C) Dulbecco's phosphate buffered saline without calcium or magnesium (DPBS).

To collect and enumerate NRel, 16 h NTHI biofilms were gently washed, then incubated with 11 μg rabbit polyclonal IgG derived from anti-rsPilA antiserum (generated against rsPilA expressed by NTHI strain

86-028NP) [30] for 6 h ('anti-rsPilA NRel') or 5.0 μg rabbit polyclonal IgG derived from anti-native IHF antiserum (generated against native IHF expressed by NTHI strain 86-028NP) [30] for 15 min ('anti-IHF NRel'), antibodies were diluted in pre-warmed equilibrated (37 °C, 5% CO_2) sBHI. These amounts of IgG match the IgG concentration present within a 1:50 dilution of each respective rabbit hyperimmune serum we used in previous studies [29,48]. The incubation times used coincide with the time wherein maximal release of NTHI from biofilm residence is achieved [29,30]. Rabbit polyclonal IgG derived from anti- NTHI OMP P5 or that isolated from naive rabbit serum served as negative controls and were used at equivalent concentrations to the NRel-inducing antisera (e.g. either 11 μg when compared to anti-rsPilA or 5 μg when compared to anti-IHF). Rabbit polyclonal IgG was generated by passage of whole serum or antiserum through rProtein A Protein G GraviTrap columns per manufacturer's instructions (GE Healthcare Life Sciences, Chicago, IL). After incubation for either 6 h (anti-rsPilA NRel) or 15 min (anti-IHF NRel), 190 μl of supernatant above the biofilm was gently collected from each well, sonicated for 2 min in a water bath sonicator to break up any aggregated NTHI, then serially diluted and plated on chocolate agar to quantitate CFU NTHI.

Sample preparation for LC-MS/MS

Anti-rsPilA NRel and anti-IHF NTHI were collected as described above. Planktonic NTHI were incubated statically in sBHI until mid-log phase of growth. Samples were centrifuged for 4 min at 13,200×*g*, resuspended in 1 ml DPBS and centrifuged again. Pellets were flash frozen and stored at −80 °C. All further processing was done by MS Bioworks, LLC (Ann Arbor, MI) as described next.

Cell pellets were suspended in buffer (2% sodium dodecyl sulfate, 150 mM NaCl, 50 mM Tris pH 8), lysed with a sonic probe (Q Sonica, Newtown, CT) and heated at 100 °C for 10 min. Protein concentration of the extract was determined by Qubit fluorometry, and 10 μg of each sample was processed by SDS-PAGE using a 10% Bis Tris NuPage mini-gel (Invitrogen) in the MES buffer system. The migration windows (1 cm gel lane) were excised and digested in-gel with trypsin using a ProGest robot (DigiLab, Hopkinton, MA) with the following protocol: 1) wash with 25 mM ammonium bicarbonate followed by acetonitrile; 2) reduce with 10 mM dithiothreitol at 60 °C followed by alkylation with 50 mM iodoacetamide at room temperature; 3) digest with trypsin (Promega, Madison, WI) at 37 °C for 4 h; 4) quench with formic acid. Supernatants were analyzed directly without further processing.

Mass spectrometry

Half of each pooled fraction was analyzed by nano LC-MS/MS with a Waters M-Class HPLC system interfaced to a ThermoFisher Fusion Lumos mass spectrometer. Peptides were loaded on a trapping column and eluted over a 75 μm analytical column at 350 nL/min; both columns were packed with Luna C18 resin (Phenomenex, Torrance, CA). The mass spectrometer was operated in data-dependent mode, with MS and MS/MS performed in the Orbitrap at 60,000 FWHM (full width at half maximum) resolution and 15,000 FWHM resolution, respectively. The instrument was run with a 3 s cycle for MS and MS/MS. Two hours of instrument time was employed for the analysis of each sample.

Mass spectrometry data processing

Data were searched using a local copy of Mascot (Matrix Science) with the following parameters: enzyme, trypsin/P; database, https://www.ncbi.nlm.nih.gov/nuccore/CP000057.2 (concatenated forward and reverse plus common contaminants); fixed modifications, carbamidomethyl (C); variable modifications: acetyl (N-term), deamidation (N,Q), oxidation (M), pyro-glu (N-term Q); mass values, monoisotopic; peptide mass tolerance, 10 ppm; fragment mass tolerance, 0.02 Da; maximum missed cleavages, 2. Mascot DAT files were parsed into Scaffold (Proteome Software) for validation, filtering and to create a non-redundant list per sample. Data were filtered using a 1% protein and peptide false discovery rate (FDR), requiring at least two unique peptides per protein. We used the normalized spectral counts for downstream analysis. To evaluate the variation and reproducibility in the replicates, we generated the PCA plot with 95% confidence ellipses surrounding each population (using the *FactoMineR* and *ggplot2* packages in R), with the normalized spectral counts for each protein identified by mass spectrometry in the three samples of planktonic, anti-rsPilA NRel, and anti-IHF NRel groups [60,61].

Differential expression analysis

Normalized spectral counts from three biological replicates of the three sample groups (planktonic, anti-rsPilA NRel and anti-IHF NRel), were used for pairwise comparisons to determine the differential expression of each protein using a two-tailed *t*-test. The *P*-values, Benjamini-Hochberg adjusted *P*-values, and fold changes are provided (Supplementary data set 1). Proteins with >1.5-fold increase or decrease and with an associated $P < 0.05$ were considered to be significantly different in expression. NTHI strain 86-028NP proteins were annotated by Clusters of Orthologous Groups of proteins [62,63].

Antibiotic sensitivity of biofilm-resident, planktonic or NRel NTHI

As we had hypothesized that NRel would be more sensitive than planktonic NTHI to certain antibiotics, we set the baseline for planktonic killing to 25% so that we would be able to demonstrate a dynamic range in NRel killing by a given antibiotic. To avoid excessive manipulation or dilution of NRel NTHI, and to permit direct comparison of equal numbers of planktonic and NRel, we adjusted the planktonic cell density to the same CFU per ml as the NRel population in each experiment as follows: NTHI were incubated statically to mid log phase growth then diluted to either 3×10^8 CFU/ml for comparison with anti-rsPilA NRel collected at 6 h, or to 2×10^8 CFU/ml for comparison with anti-IHF NRel collected at 15 min (see Fig. 1). We then determined the concentrations of amoxicillin (Sigma-Aldrich, St. Louis, MO) and clavulanate (U.S. Pharmacopeia, Rockville, MD), or of trimethoprim (Sigma-Aldrich) and sulfamethoxazole (Santa Cruz Biotech, Dallas, TX) that killed approximately 25% of planktonic NTHI at each density. The same antibiotic concentrations were used for the anti-IHF or anti-rsPilA NRel, the density-matched (same CFU/ml) planktonic NTHI, and the adherent biofilm for each relevant experiment. Likewise, for anti-IHF or anti-rsPilA NRel collected at 2 h, we first quantitated NRel, and found $\sim 2.0 \times 10^8$ or 4.0×10^8 CFU/ml released by exposure of biofilms to anti-rsPilA or anti-IHF IgG, respectively. We then assessed killing of anti-IHF or anti-rsPilA NRel by concentrations of amoxicillin plus clavulanic acid ("augmentin", AMC) or trimethoprim plus sulfamethoxazole (TMP-SMX) that killed 25% of the planktonic NTHI at the same density.

Anti-rsPilA or anti-IHF NRel were collected and sonicated as described above. After sonication for 2 min in a water bath sonicator to break up any NTHI aggregates, NRel or planktonic NTHI were incubated with the indicated antibiotics at 37 °C for 2 h, then serially diluted and plated on chocolate agar to quantify viable NTHI. To assay biofilm-resident NTHI, biofilms were established for 16 h at 37 °C as described above, washed twice with DPBS and incubated in sBHI supplemented with the indicated antibiotics at 37 °C. After 2 h, biofilm-resident NTHI were collected by forceful pipetting, sonicated for 2 min and enumerated as described above. All experiments were performed at least three times on separate days with two or three technical replicates for each treatment and control group.

Flow cytometry

As described above, NTHI biofilms were established in 8-well chambered coverglass slides. After 16 h, medium was aspirated from each well

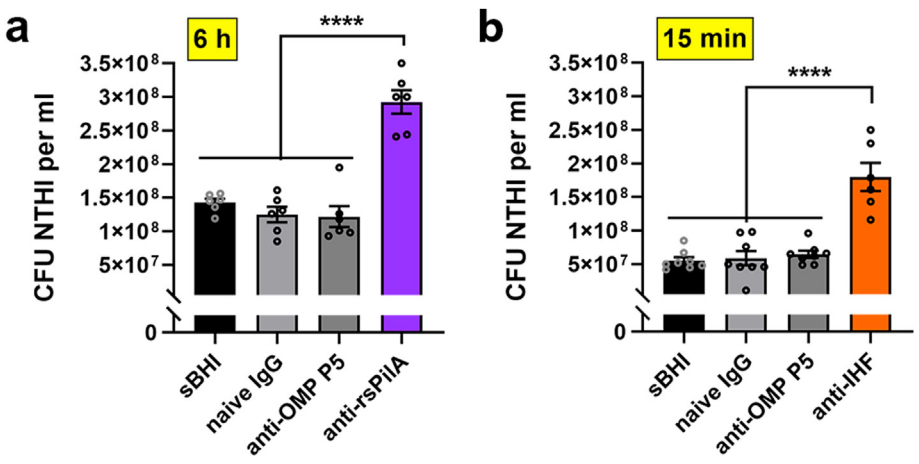

Fig. 1. Quantitation of NTHI released from biofilm-residence by either anti-rsPilA or anti-IHF. NTHI biofilms established for 16 h were incubated for an additional **(a)** 6 h with rabbit anti-rsPilA IgG or **(b)** 15 min with rabbit anti-IHF IgG or with each of three negative controls (sBHI, IgG isolated from naive serum or IgG isolated from anti-OMP P5 serum) followed by quantitation of NTHI recovered from supernatants above the biofilms. Anti-rsPilA and anti-IHF induced significant release of NTHI from biofilm residence into the NRel state. Individual data points are shown, bars represent mean ± SEM.****, $P < 0.0001$, One-way analysis of variance with the Holm-Sidak correction.

and biofilms incubated with 5 μg IgG from rabbit polyclonal IHF for 15 min or 11 μg IgG from polyclonal rabbit anti-rsPilA for 6 h at 37 °C, 5% CO_2. At each respective timepoint, 190 μl of supernatant above each biofilm was collected, transferred into 1 μM FM1-43FX (Invitrogen, Carlsbad, CA) in Hank's Balanced Salt Solution and incubated static for 15 min at room temperature. NTHI scraped from a chocolate agar plate into buffer served as a 'clumped' bacterial control. NTHI suspended in buffer by gentle pipetting followed by sonication for 5 min served as a 'non-clumped' bacterial control. Forward scatter and side scatter profiles of fluorescently stained NTHI were examined with a BD LSR II flow cytometer and FloJo software. 10,000 events were collected for each sample.

RNA isolation and qRT-PCR assay

For RNA isolation, we seeded 6 ml of NTHI at 2×10^5 CFU/ml into a T-25 tissue culture flask. After 16 h incubation at 37 °C, 5% CO_2, the flask was gently inverted, and the medium poured off. With the flask upside down, 6 ml prewarmed DPBS was added then the flask was slowly inverted to gently wash the biofilm. To remove the DPBS wash, the flask was inverted again and DPBS poured off. Antibody diluted in sBHI was added with the flask still upside down, to deliver the same concentration of antibody/cm^2 as used in chamberslide assays [this translated to ~52 μg anti-IHF IgG per ml or ~113 μg anti-rsPilA IgG per ml]. The flask was returned to the incubator, inverted gently so that the medium again covered the biofilm. After 3 min for anti-IHF, or 3 h for anti-rsPilA, the flask was inverted and the NRel NTHI collected by pouring into a 15 ml conical tube. NRel were centrifuged for 1 min at 16,000×*g*, the supernatant aspirated, and 1 ml TRIzol™ Reagent (ThermoFisher, Waltham, MA) was immediately added to the bacterial pellet. Samples were stored at −80 °C.

RNA was purified with a Qiagen RNeasy kit (Qiagen, Germantown, MD). Residual DNA was removed by treatment with DNase I (NEB, Ipswich, MA), per manufacturer's instructions for 45 min at 37 °C in the presence of 20 U SUPERase In RNase inhibitor (Ambion, Austin, TX). Relative gene expression was assessed by quantitative reverse transcription-PCR (qRT-PCR) with a Superscript III Platinum SYBR Green One-Step qRT-PCR kit (ThermoFisher) per manufacturer. Gene expression was normalized to *16S*, and relative expression was calculated by the comparative ($\Delta\Delta C_T$) method, with fold change in gene expression expressed as $2^{(-\Delta\Delta CT)}$. Results represent the mean of 3 biological samples, each assayed in triplicate. A 2-fold change in gene expression was considered biologically significant. Primers used are listed in Table 1.

Statistical analyses

Data are expressed as mean ± SEM of at least three biological replicates performed on separate days with two or three technical replicates per sample. Statistical analyses were performed with GraphPad (Prism) software version 8.2. Multiple comparisons were made by one-way analysis of variance with the Holm-Sidak correction. All other comparisons were made with student's *t*-test. Comparisons of fold changes in normalized spectral counts of proteins identified by mass spectrometry and generation principal component analysis were performed in R (Bioconductor). Flow cytometry data were analyzed by the Kolmogorov-Smirnov test to compare the cumulative distribution of anti-rsPilA NRel versus anti-IHF NRel for forward scatter and side scatter profiles.

Table 1
Primers used in this study.

Primer	Sequence
acrR-forward	CGGCGATAAATTTAGCCTCTGA
acrR-reverse	TGAATCGCACGCCAAGAG
artM-forward	GTCTTATCCAATGCGTGGTTCT
artM-reverse	GGATGCTAATGCCGTTCCTTTA
deaD-forward	TGTGGTGAACTACGACATTCC
deaD-reverse	GATCCTGATCGGCTGTGAATAA
emrA-forward	CCGCAAATACAGAATGCGATAAA
emrA-reverse	ATTACGACGCGCCACATAG
emrB-forward	CGGTAACTTTCGAGCCATCA
emrB-reverse	GCCAGACAGCGTTATTGTAGTA
fis-forward	TAATCCTGCCGATGCCTTAAC
fis-reverse	CGGGTTTGATTACCACGAGTAT
folA-forward	TTGGTCGTCCACTACCTAAAC
folA-reverse	GACCGCACTTTCAAAGCTATC
folP-forward	TGCTGGATTTCTGTCGATTCTT
folP-reverse	GCTCTTGCAAAGCACGAATATC
16S-forward	AAAGGAGACTGCCAGTGATAAA
16S-reverse	CCCTCTGTATACGCCATTGTAG

Data availability

All data generated or analyzed during this study are included in this published article and its supplementary information files (Suppl. Table 1 & Suppl. Dataset 1).

Results

Incubation of NTHI biofilms with anti-rsPilA or anti-IHF antibodies released NTHI from biofilm residence

Anti-rsPilA antibodies specifically target PilA, the majority subunit of NTHI T4P [33], to induce a more gradual, top-down release of NTHI from the biofilm which we refer to as '*dispersal*' as this is a programmed process that requires active NTHI participation by expression of both T4P and AI-2-dependent signaling [33]. In contrast, anti-IHF antibodies

induce a rapid, non-programmed, species-independent, biofilm matrix collapse with immediate release of bacteria *en masse*, we refer to as '*disruption*' [45,48]. This latter outcome does not require bacterial action Table 2 [32,43–45]. To now expand further on this understanding, we first quantified the number of NTHI released from biofilm residence after incubation with rabbit polyclonal IgG isolated from either anti-rsPilA or anti-IHF serum. Sterile culture medium or an equivalent concentration of polyclonal IgG recovered from either naive serum or from antiserum against the NTHI adhesin outer membrane protein P5 (OMP P5), none of which disperse established NTHI biofilms [29,33], served as negative controls. Our prior work reveals that NTHI biofilms established for 16 h and incubated with anti-rsPilA are maximally dispersed after 6 h [29,33], whereas complete collapse of a similarly aged biofilm is achieved after 15 min with anti-IHF [49]. Thus, for this assay, NRel induced by anti-rsPilA or anti-IHF were collected for enumeration at either 6 h or 15 min, respectively [29,33,49].

The concentration of NTHI recovered from supernatants above biofilms that had been incubated with polyclonal IgG from either naive or anti-OMP P5 serum was similar to that when incubated with sterile sBHI [Fig. 1a and b]. This was anticipated as none of these three treatments were expected to significantly alter the normal equilibrium wherein bacteria go on/come off a biofilm as a natural part of biofilm growth and remodeling within the 6 h or 15 min incubation periods. Conversely, incubation with anti-rsPilA IgG for 6 h induced a significant >2-fold increase in the concentration of released NTHI (Fig. 1a, $P < 0.0001$). Similarly, incubation with anti-IHF IgG for 15 min resulted in a significant >3-fold increase in concentration of released NTHI ($P < 0.0001$) [Fig. 1b]. The lower concentration of the 3 control populations, compared to those similarly depicted in Fig. 1a, reflects the shorter 15 min incubation period. We refer to these populations of NTHI newly released from biofilm-residence as 'anti-rsPilA NRel' or 'anti-IHF NRel' to reflect their generation due to the action of two unique and specifically-targeted antibodies wherein the mechanisms and kinetics of release of biofilm resident NTHI are different [Table 2].

FACS analysis of anti-rsPilA and anti-IHF NRel populations

As hypothesized and based on gross observations of the NRel populations as they were recovered, the scatter profiles for anti-rsPilA NRel and anti-IHF NRel are also distinct. We performed flow cytometry and examined the forward scatter and side scatter profiles for each NRel population to reveal potential differences in size and complexity. The scatter profile for a suspension of NTHI that was briefly sonicated prior to assessment revealed a population of cells of similar size (i.e. single cells), whereas a larger and more complex population (i.e. aggregates) was additionally observed in the sample with bacterial aggregates, indicated by greater side scatter and forward scatter [Fig. S1, **panel a**]. Anti-rsPilA NRel appear to be released as individual cells [Fig. S1, **panel b**], as a single, uniform population was revealed. Conversely, the scatter profile for anti-IHF NRel included a larger population, indicative of bacterial aggregates and/or biofilm remnants [Fig. S1, **panel c**]. Moreover, the anti-IHF NRel population was 10% larger in size [Fig. S1, **panel d**] and 47% more complex [Fig. S1, **panel e**] compared to the anti-rsPilA NRel, further evidence of distinct character of each population. Moreover, these data fit well with the described differences for how each antiserum mediates release of NTHI from biofilm residence (Table 2) as the programmed release mediated via dispersal would indeed favor release as individual cells, whereas the rapid physical collapse of the biofilm to release NTHI via disruption would favor release as aggregates.

Table 2
Differences between mechanisms of NTHI release from biofilm-residence to the NRel state as mediated by anti-rsPilA or anti-IHF.

	anti-rsPilA	anti-IHF
Antigen location	NTHI surface [22]	Biofilm structural linchpin [45]
NTHI contribution	Active - native/ programmed [33]	Passive - artificially induced
Release speed	Slow [33]	Fast [48]
Release mode	Top-down [33]	All at once [49]
NTHI-specific antigen?	Yes	No, species-agnostic [45]
NRel in lag phase?	No (this study)	Yes (this study)
Released as aggregates?	No (this study)	Yes (this study)
Term used to define release from biofilm	*Dispersal*	*Disruption*

Proteomic expression profiles of anti-rsPilA and anti-IHF NRel were distinct from both their planktonically grown counterparts and importantly, from each other

Given our ultimate interest in the relative sensitivity of NRel NTHI to killing by antibiotics, next we questioned how the anti-rsPilA and anti-IHF NRel populations compared phenotypically to not only planktonically grown NTHI (the population used clinically to determine antibiotic sensitivities, or MIC values), but also to each other. To begin to address this central question, we examined the proteomic expression profiles of anti-rsPilA NRel, anti-IHF NRel and planktonic NTHI (grown statically in broth to mid-log phase) by mass spectrometric analysis. The total proteomic expression profiles for anti-rsPilA and anti-IHF NRel were different from planktonic NTHI, as shown by the discrete locations of each population on the principal component analysis (PCA) plot [Fig. 2a]. Moreover, although we had anticipated that NRel population proteomic profiles would be different from planktonic cells [29,48], the two NRel populations were also very different from each other, as highlighted by the 95% confidence ellipses, despite genetic identity.

Due to the overall global changes in protein expression between the anti-rsPilA or anti-IHF NRel and planktonically grown NTHI, we next examined proteins with differences in abundance between the two NRel populations, after each was first compared to planktonic NTHI. There was a total of 63 and 103 differentially expressed proteins (DEPs) with a significant >1.5-fold increase or decrease in abundance compared to planktonic NTHI ($P < 0.05$) in anti-rsPilA NRel and anti-IHF NRel populations, respectively [Fig. 2b & Suppl. Table 1]. Moreover, anti-rsPilA NRel expressed 40 proteins and anti-IHF NRel expressed 80 proteins with uniquely significant differences in abundance compared to planktonic NTHI, which provided further evidence of the difference between the two NRel populations [Fig. 2b**,** purple versus orange sections].

We next annotated the DEPs by Clusters of Orthologous Groups of proteins (COG) [62,63] to assess the relative functions of the two NRel DEPs as a result of release from biofilm residence via distinct antibody-mediated dispersal versus disruption. For the anti-rsPilA NRels, annotation of the 63 DEPs revealed that the most frequently represented COG categories (36.5%) were involved in either energy production & conversion (19.0%) or amino acid transport & metabolism (17.5%) [Fig. 2c, purple bars & Suppl. Table 1]. Specific to energy production & conversion category, enzymes involved in glycolysis, tricarboxylic acid cycle, nitrogen metabolism, and anaerobic metabolism of glycerol were >1.5-fold decreased in abundance compared to planktonic NTHI. Whereas proteins involved in lactate uptake and utilization were >1.5 fold increased in abundance compared to planktonic NTHI [Suppl. Table 1]. In the same category, DEPs specific to anti-rsPilA NRel with >1.5-fold increase included tryptophan biosynthesis and cysteine metabolism enzymes. The collective differences in protein functional categories indicated that anti-rsPilA NRel were primarily in an active-adaptive energy utilization and amino acid metabolic state.

In contrast, within the anti-IHF NRel population, 'translation, ribosomal structure & biogenesis' was the most frequently represented COG category (13.6%) among the 103 DEPs, compared to planktonic NTHI [Fig. 2c, orange bars & Suppl. Table 1]. Specific to anti-IHF NRel DEPs, eight were 30S and 50S ribosomal proteins with >1.5-fold increase, and although ribosomal structural proteins were also increased, two translation initiation factors were decreased >1.5-fold [Suppl. Table 1].

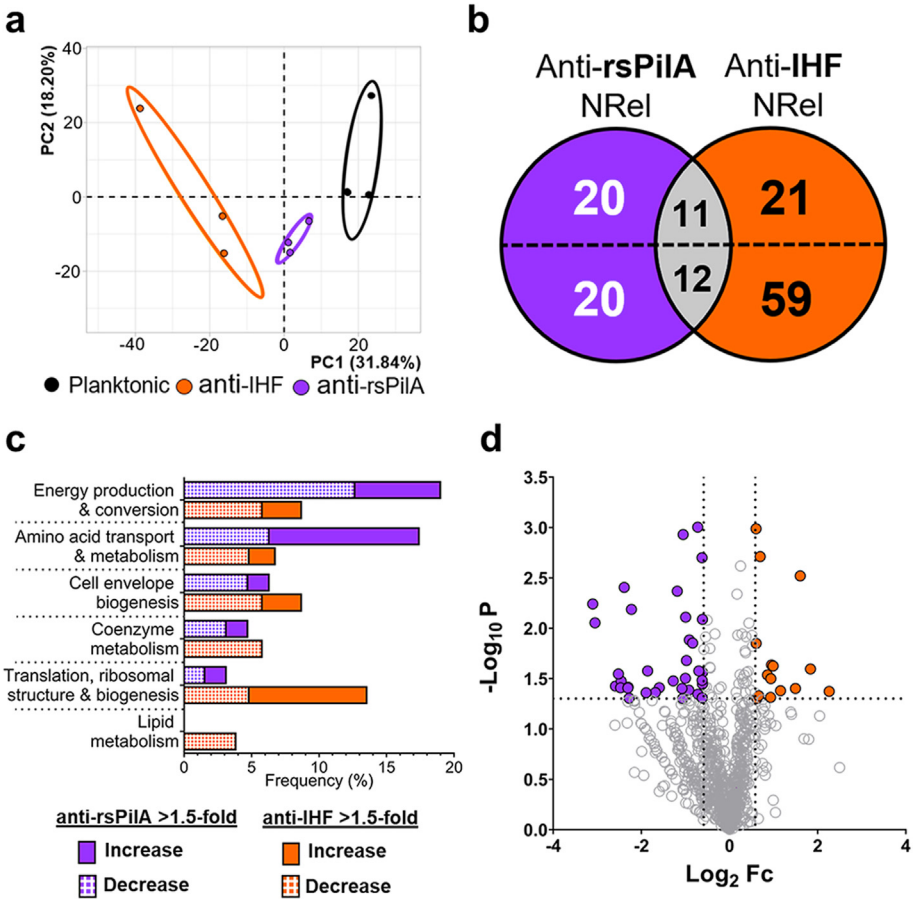

Fig. 2. Release of NTHI from a biofilm by incubation with anti-rsPilA or anti-IHF antibodies generated NRel populations with distinct proteomic expression profiles compared to planktonically grown NTHI and, importantly, to each other. **(a)** Principal component analysis (PCA) plot generated from the normalized spectral counts of each protein in anti-rsPilA NRel (purple dots), anti-IHF NRel (orange dots) and planktonically grown NTHI (black dots). Triplicate samples of each population are encircled by 95% confidence ellipses. The proteomic expression profiles of anti-rsPilA and anti-IHF NRel were distinct from both planktonically grown NTHI, and from each other. **(b)** Venn diagram of the number of proteins with a significant ($P < 0.05$) 1.5-fold increase (above the dashed line) or decrease (below the dashed line) specific to anti-rsPilA (purple), anti-IHF (orange), or shared (gray), compared to planktonic NTHI. **(c)** The anti-rsPilA (purple bars) and anti-IHF (orange bars) NRel demonstrated distinct protein expression patterns with a significant ($P < 0.05$) 1.5-fold increase or decrease represented by different COG categories when compared to planktonically grown NTHI. **(d)** Direct comparison of differences in protein expression profiles of anti-IHF and anti-rsPilA NRel populations with a significant ($P < 0.05$) 1.5-fold increase or decrease compared to each other, as shown by a volcano plot of anti-IHF NRel versus anti-rsPilA NRel. Negative significant fold decreases represent proteins with greater abundance in the anti-rsPilA NRel (purple dots), while positive fold increases represent greater protein abundance in the anti-IHF NRel (orange dots) compared to each other. (For interpretation of the references to colour in this figure legend, the reader is referred to the Web version of this article.)

Further, expression of each of the cell envelope biogenesis, coenzyme metabolism, and lipid metabolism COG category proteins were >1.5-fold decreased compared to planktonic NTHI, for example, Lic2A, LicC, and LicD, proteins responsible for modification of lipooligosaccharide (LOS) and decoration with a phosphorylcholine moiety [64,65], and the lipoprotein carrier protein LolA, which shuttles lipoproteins from the inner membrane to the outer membrane [66]. Moreover, there were four anti-IHF NRel DEPs within the lipid metabolism category which were significantly >1.5-fold decreased in expression compared to planktonic NTHI [Fig. 2c]. Additionally, coenzyme metabolism proteins required for biosynthesis of biotin, a cofactor in fatty acid biosynthesis, were also significantly >1.5-fold decreased in expression [67]. In contrast, the outer membrane lipoprotein OMP P6, involved in maintenance of outer membrane integrity and attachment to peptidoglycan, and the major outer membrane protein OMP P2 were significantly increased in expression compared to planktonic NTHI [Suppl. Table 1] [68,69]. Collectively, these data suggested that anti-IHF NRel contained abundant ribosomes for translation of proteins, however translation was limited due to the reduced translation initiation factor proteins. Further, anti-IHF NRel demonstrated decreased expression of LOS-modifying enzymes and lipid metabolism genes, with a concurrent increase in expression of outer membrane integrity maintenance proteins, which suggested differences in membrane composition of anti-IHF NRel compared to planktonically grown NTHI.

The increased abundance of ribosomal proteins observed in the anti-IHF NRel proteomic profile is also characteristic of bacteria in lag phase of growth [70]. To determine whether anti-IHF NRel showed other similarities with lag phase bacteria, we used qRT-PCR to examine the expression of three genes canonically expressed by bacteria in lag phase [70]. Expression of *deaD, artM,* and *fis* was significantly (>2-fold) upregulated in anti-IHF NRel *vs.* planktonic NTHI (Fig. S2a). Interestingly, for all three of these genes, the fold increase in transcript abundance over planktonic NTHI was significantly greater for anti-IHF *vs.* anti-rsPilA NRel ($P < 0.05$). Thus, that anti-IHF NRel appeared to be released from biofilm residence in a state which mimicked lag phase, presented another significant difference between the anti-IHF and anti-rsPilA phenotypes (Table 2), and again suggested that physical collapse of the biofilm structure resulted in rapid release while NTHI was metabolically more quiescent than anti-rsPilA NRel.

Because the proteomic expression profiles of the two NRel populations were different from each other [Fig. 2a], we next conducted a direct comparison of DEPs between the two NRel populations as depicted by volcano plot [Fig. 2d]. Fifty-one DEPs with >1.5-fold increase or decrease were identified amongst anti-IHF NRel versus anti-rsPilA NRel [Fig. 2d & Suppl. Table 1]. Of these, 15 proteins (29.4%) demonstrated a >1.5-fold increase in expression by anti-IHF NRel compared to anti-rsPilA NRel, and these proteins included five of the 30S and 50S ribosomal proteins described prior. Also, OMP P6 was more abundant in anti-IHF NRel compared to anti-rsPilA NRel. DEPs with a >1.5-fold decrease in the anti-IHF NRel compared to anti-rsPilA NRel (e.g. greater abundance in anti-rsPilA NRel) were characteristic of the abundantly expressed tryptophan biosynthesis proteins. These distinctions were in addition to relative differences in lipid metabolism proteins that had already been identified as decreased in expression in the anti-IHF NRel population compared to planktonic NTHI. Notably, this direct comparison of the two NRel proteomic expression profiles also revealed a significant increase in the peptidoglycan synthesis protein, MurB [71], within the anti-IHF NRel DEPs compared to anti-rsPilA NRel, which further suggested the altered cell envelope composition of the anti-IHF NRels [Suppl. Table 1].

Anti-rsPilA or anti-IHF NRel were significantly more sensitive to killing by a specific antibiotic than planktonic NTHI

With the observed significant differences in relative expression of distinct proteins between the two NRel populations demonstrated, we next examined how these differences altered phenotypic character. As bacteria newly released from a biofilm are typically more sensitive to killing by antibiotics than their planktonic counterparts [29,48,54,55], we assessed the sensitivity of NRel NTHI to TMP-SMX or to AMC, as these represent antibiotics commonly prescribed for NTHI-induced OM and respiratory infections [72–78]. We compared the anti-rsPilA NRel and anti-IHF NRel susceptibilities to killing by TMP-SMX or AMC, to that of both biofilm-resident NTHI (canonically highly resistant) and to planktonic NTHI grown to mid-log phase of growth (canonically sensitive and representative of the population commonly used to determine MIC values in clinical microbiology laboratories) [Fig. 3a]. To control for differences in the numbers of NTHI released by exposure to anti-IHF IgG for 15 min or by anti-rsPilA IgG for 6 h (see Fig. 1), we adjusted the density of the planktonic NTHI in each experiment to match that of either the anti-IHF or anti-rsPilA NRel population. After we identified the concentrations of AMC or TMP-SMX needed to reproducibly kill ~25% of planktonic NTHI at each bacterial density, we then used these concentrations to assess relative killing of the corresponding NRel or biofilm-resident NTHI.

As expected, anti-rsPilA NRel were significantly more sensitive than biofilm-resident NTHI to killing by either TMP-SMX or AMC ($P \leq 0.0001$) [Fig. 3b&c]. Notably however, sensitivity of anti-rsPilA NRel to killing by TMP-SMX was significantly greater compared to that for planktonic NTHI ($P \leq 0.001$) after only 2 h of antibiotic exposure [Fig. 3b]. In contrast, anti-rsPilA NRel were only equally as sensitive as their planktonic counterparts to killing by the β-lactam antibiotic AMC [Fig. 3c]. We then similarly evaluated anti-IHF NRel and found that they too were significantly more sensitive than biofilm-resident NTHI to killing by either TMP-SMX or AMC ($P \leq 0.0001$), again as expected [Fig. 3d&e]. Intriguingly however, and in direct contrast to anti-rsPilA NRel, the anti-IHF NRel population was only equally as sensitive to TMP-SMX mediated killing as their planktonic counterparts [Fig. 3d], but significantly more sensitive to AMC ($P \leq 0.0001$) [Fig. 3e].

Bacterial sensitivity to antibiotic killing is the result of multiple processes that include drug uptake, efflux, and degradation, as well as the direct mechanism of antibiotic action [79]. To identify possible mechanisms for the selectively enhanced antibiotic sensitivities of anti-IHF or anti-rsPilA NRel, we used qRT-PCR to examine the relative expression of several genes likely to play a role in susceptibility or resistance to TMP-SMX or AMC. The protein targets of TMP and SMX, dihydrofolate reductase and dihydropteroate synthetase, are encoded by *folA* and *folP*, respectively; overproduction of FolA and FolP is associated with resistance to TMP-SMX [80]. Accordingly, we speculated that anti-rsPilA NRel NTHI would likely demonstrate less relative expression of *folA* and/or *folP* than anti-IHF NRels at the selected time points. Our results confirmed this hypothesis, as *folA* and *folP* expression were both significantly reduced in anti-rsPilA *vs.* anti-IHF NRel (Fig. S2b, $P < 0.0001$).

Efflux pumps enable bacteria to decrease the concentration of intracellular antibiotic. The EmrE efflux system transports β-lactam antibiotics in *Neisseria gonorrhoeae* [81], and in *E. coli*, TMP-SMX exposure stimulates expression of the EmrAB efflux pump [82], which suggested that the EmrAB efflux pump could influence NRel sensitivity to TMP-SMX. We found that relative expression of *emrA* and *emrB* by anti-rsPilA NRel was significantly less that by anti-IHF NRel, consistent with the greater sensitivity of anti-rsPilA NRel to TMP-SMX (Fig. S2c, $P < 0.001$). In contrast, the ArcAB efflux pump can transport β-lactam antibiotics and is under the control of the transcriptional repressor *acrR* [83]. While enhanced AcrAB expression via *acrR* mutations has been linked to amoxicillin resistance in *Haemophilus* (https://aac.asm.org/content/51/7/2564.long), we argue that enhanced expression of *acrR* would likely have the opposite effect, enhanced susceptibility of NTHI to AMC. As we anticipated, relative *acrR* expression was significantly greater by anti-IHF *vs.* anti-rsPilA NRel, consistent with the heightened sensitivity to AMC observed for anti-IHF NRel (Fig. S2c, $P < 0.0001$).

Taken together, our antibiotic sensitivity and transcript abundance data suggested that anti-rsPilA and anti-IHF NRel differed significantly in their relative antibiotic sensitivities due to the mechanism by which they were released from biofilm residence. However, we were concerned that the difference in time required for maximal disruption (minutes) *vs.* dispersal (hours) might have also played a role in the observed phenotype. Thereby, we repeated our analysis of relative antibiotic sensitivities on time-matched NRel populations recovered after incubation with either anti-rsPilA or anti-IHF IgG for 2 h, a timepoint approximately midway between the times of maximal release for both antibodies. Similar to the results shown in Fig. 3, anti-rsPilA NRel were significantly more susceptible to killing by TMP-SMX ($P \leq 0.0001$) (Fig. 4a), and equally susceptible to killing by AMC, as planktonic NTHI (Fig. 4b). Moreover, time-matched anti-IHF NRel were again equally susceptible to killing by TMP-SMX (Fig. 4c) and significantly more susceptible to killing by AMC ($P \leq 0.0001$) (Fig. 4d), compared to planktonic NTHI. These results provided further support for our hypothesis that the distinct antibiotic sensitivity phenotypes shown resulted from the two different mechanisms of release, dispersal *vs.* disruption.

To date, we have shown extensive differences between the two mechanisms and outcomes of anti-rsPilA or anti-DNABII antibody-mediated release of biofilm-resident bacteria to the NRel state (Table 2). New data presented here added additional phenotypic distinctions between anti-rsPilA and anti-IHF NRel, wherein these two genetically identical populations exhibited not only distinctive proteomic and targeted transcriptomic expression profiles but also revealed that they were released from biofilm residence in distinct phases of growth and further, were released as either aggregates vs. as individual cells. Moreover, the two NRel populations demonstrated significantly increased, but different susceptibilities to killing by either a sulfonamide or a β-lactam antibiotic when compared to planktonic NTHI, both of which are first-line antibiotics recommended for treatment of NTHI-induced diseases.

Discussion

Historically, the development paths for vaccines and those for antibiotics have proceeded in parallel, with one focused on prevention and the other on treatment [84]. Whereas this strategy has indeed been successful for many diseases, we now face the issue of multiple chronic and recurrent infections for which neither path has yet achieved overall success. There are widely acknowledged obstacles to progress in this regard, none the least of which is the typically inherently slow vaccine development process [85]. Similarly, there are tremendous challenges to the antibiotic development pathway, with no clinically approved truly new class of drug introduced for >30 years, despite extensive effort necessitated by a worrisome rapid increase in the rise of multi-antibiotic resistant bacteria worldwide [86,87]. These obstacles to progress are understandable given the complex and difficult-to-treat nature of chronic diseases, which has confounded both discovery pathways. Such persistent and recurrent infections are attributable to causative agents that form biofilms wherein the resident bacteria have a unique transcriptome and a highly recalcitrant phenotype that renders them resistant to antibiotics and host immune effectors that readily kill their planktonic counterparts [4,6,88–91]. Our advances in the recognition and understanding of the NRel phenotype now provide us with the opportunity to merge aspects of these development pathways to consider the use of therapeutic antibodies to release bacteria from the recalcitrant biofilm-residence into a state that is now markedly more vulnerable to killing.

In our previous studies, we showed that established NTHI biofilms concurrently exposed to both antiserum against a bacterial DNABII protein and an antibiotic were significantly more sensitive to killing by three antibiotics commonly used to treat OM (e.g. ampicillin, AMC and cefdinir) at concentrations ≥4-fold below the MIC, compared to their planktonic counterparts [48]. We also showed that both NRel NTHI and NRel

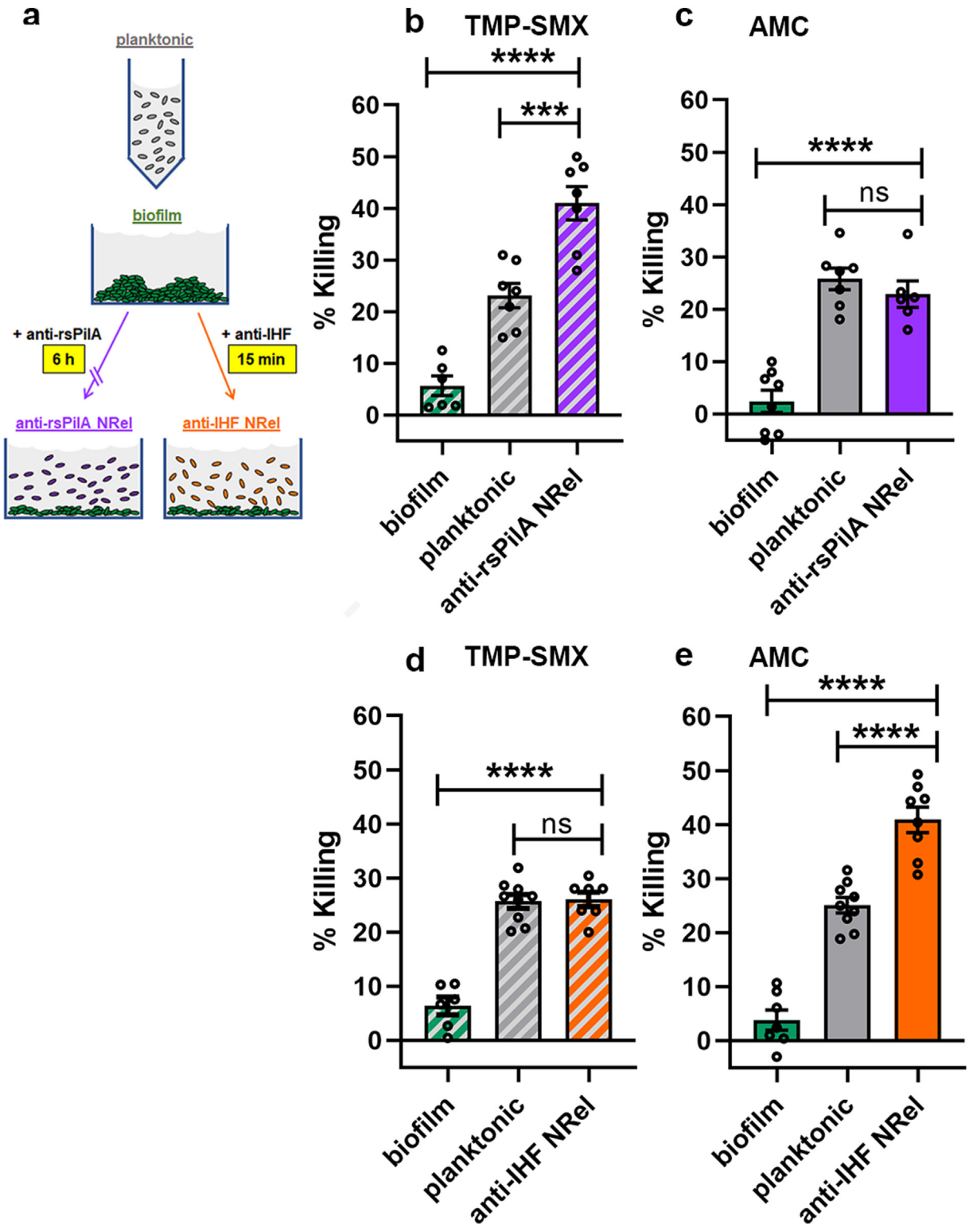

Fig. 3. NRel NTHI populations were more sensitive to killing than their planktonic counterparts, and this sensitivity was distinct from each other. **(a)** Diagram of the four populations of NTHI tested herein. NRel were generated by incubation of NTHI biofilms with rabbit polyclonal IgG isolated from anti-rsPilA serum (6 h, purple) or from anti-IHF serum (15 min, orange). **(b&c)** Anti-rsPilA NRel were significantly more sensitive to killing by trimethoprim/sulfamethoxazole than planktonic NTHI (TMP-SMX at 0.94 μg and 4.7 μg per ml respectively, panel b), but only equally as sensitive to killing by amoxicillin/clavulanate (AMC at 2.5 μg and 1.25 μg per ml, respectively panel c). Biofilm-resident NTHI displayed minimal sensitivity to either TMP-SMX or AMC as expected. **(d&e)** In contrast, anti-IHF NRel were only equally as sensitive to killing by TMP-SMX as planktonic NTHI (0.09 and 0.45 μg/ml respectively, panel d), but significantly more sensitive to killing by AMC (0.30 and 0.15 μg/ml respectively, panel e). The uniquely heightened sensitivity of NTHI NRel to killing by either TMP-SMX or AMC was dependent upon the mechanism by which they were released from biofilm residence. Individual data points are shown, bars represent mean ± SEM. $^{***}P < 0.001$, $^{****}P < 0.0001$, one-way analysis of variance with the Holm-Sidak correction. (For interpretation of the references to colour in this figure legend, the reader is referred to the Web version of this article.)

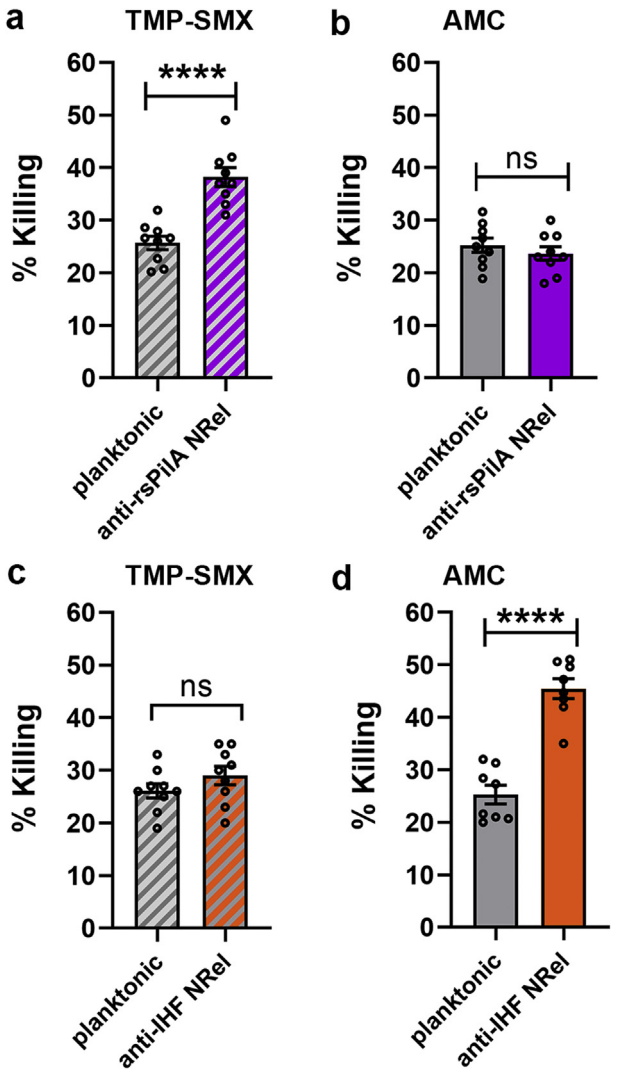

Fig. 4. Enhanced sensitivity of anti-rsPilA or anti-IHF NRel NTHI to TMP-SMX or AMC, respectively, was independent of the timing of NTHI release from biofilm residence. We exposed biofilms to rabbit polyclonal IgG isolated from either anti-rsPilA or anti-IHF serum for 2 h, then collected NRel NTHI and assayed for relative antibiotic sensitivity. **(a&b)** Anti-rsPilA NRel were significantly more sensitive to killing by TMP/SMX than planktonic NTHI (TMP-SMX at 0.09 μg and 0.45 μg per ml respectively, panel a), but only equally as sensitive to killing by AMC (AMC at 0.3 μg and 0.15 μg per ml, respectively panel b). **(d&e)** In contrast, anti-IHF NRel were only equally as sensitive to killing by TMP-SMX as planktonic NTHI (0.94 and 4.7 μg/ml respectively, panel c), but significantly more sensitive to killing by AMC (2.5 and 1.25 μg/ml respectively, panel d). These data showed that time-matched anti-rsPilA or anti-IHF NRel maintained the same distinct antibiotic sensitivity phenotype as shown when 15 min anti-IHF NRel were compared to 6 h anti-rsPilA NRel (see Fig. 3). Individual data points are shown, bars represent mean ± SEM. ****$P < 0.0001$, one-way analysis of variance with the Holm-Sidak correction.

M. catarrhalis are more susceptible to TMP-SMX or clarithromycin, respectively, when released from a dual-species biofilm by incubation with anti-rsPilA, than those from growth on agar [29]. Given our previous observations, here we aimed to begin to understand the relative phenotypes of the two NRel populations as induced by the specifically targeted anti-rsPilA and anti-IHF sera, which release NTHI from biofilm residence by discrete mechanisms as this could have a notable influence on relative clinical approach to best mediate eradication of the resultant NRel population.

In this study, we characterized anti-rsPilA and anti-IHF NRel and showed that their relative proteomic expression profiles, relative expression of targeted genes and sensitivity to killing by antibiotics were distinct not only from planktonically grown NTHI, but importantly, also from each other. Although the kinetics of release by anti–IHF–mediated disruption *vs.* anti-rsPilA-mediated dispersal are clearly different, our results strongly suggest that the observed differences in NRel phenotype were dependent on the specific antibody that mediated release from biofilm residence. The proteomic expression profiles provided a snapshot in time of the total released NRel populations. The anti-rsPilA NRel population proteomic profile was defined by an adaptive state of energy metabolism & conversion and amino acid transport & metabolism in response to their being induced to actively disperse from the biofilm. This adaptive metabolic state is likely somewhat more heterogeneous than anti-IHF NRel NTHI due to the more gradual release of cells as they actively disperse from the biofilm due to expression of both AI-2 and the Type IV twitching pilus over the 6 h incubation period. Nonetheless, the adaptive metabolic state of this anti-rsPilA NRel population was very similar to that described for other genera (e.g. *S. pneumoniae, K. pneumoniae, and P. aeruginosa)* in response to release from a biofilm and thereby does not appear to be atypical [92–94].

In analysis of the anti-IHF NRel population, we found that it was defined by an increased production of ribosomal proteins with a concurrent decrease in LOS modification, cell membrane maintenance and lipid metabolism proteins. The enrichment of ribosomal proteins suggested that the anti-IHF NRel population was poised for protein synthesis with an altered membrane composition in response to rapid passive release *en masse* into the surrounding milieu. As such, anti-IHF NRel might be expected to still largely resemble biofilm-resident NTHI bacteria. Indeed, targeted transcriptomics indicated that anti-IHF NRel were in a state of growth similar to lag phase. Nonetheless, the anti-IHF NRel phenotype was also clearly different from that of biofilm-resident NTHI, as revealed by their significantly greater killing by both sulfonamide and β-lactam antibiotics compared to biofilm-resident NTHI.

As expected from our previous work [29,48], NRel NTHI were highly sensitive to two first-line antibiotics prescribed to treat NTHI-induced diseases. However, here we showed for the first time that these NRel populations displayed unique enhanced sensitivity to killing by a different class of antibiotic dependent on whether they had been released from biofilm residence by either dispersal (e.g. via anti-rsPilA) or disruption (e.g. via anti-IHF). These differences cannot be explained by a direct effect of either anti-rsPilA or anti-IHF on NRel NTHI, since neither NTHI viability or susceptibility to killing by either of these antibiotics is affected by incubation with either antibody [29,48]. Collectively, the two resultant NRel populations showed significant differences in relative proteomic expression profiles, targeted transcriptomic profiles, character of release from biofilm residence (both growth phase and as single cells vs. aggregates), and antibiotic sensitivities.

The anti-rsPilA NRel adaptive amino acid transport & metabolism state provided insight into the mechanism of this population's uniquely increased susceptibility to TMP-SMX, because the sulfonamide class of antibiotic targets the folic acid synthesis pathway involved in amino acid synthesis [95]. Also, compared to anti- IHF NRel, the lower relative expression of *folA* and *folP,* which encode the protein targets for TMP and SMX, respectively, together with lower expression of *emrA* and *emrB*, which encode subunits of the EmrAB efflux pump that transports TMP-SMX out of the cell, also supported the greater sensitivity to TMP-SMX of anti-rsPilA *vs.* anti- IHF NRels. Similarly, the differences noted in the anti- IHF NRel lipid metabolism and cell membrane composition proteins supported the observed increased sensitivity to AMC, wherein the modified membrane content could have altered membrane permeability to allow greater access of the β-lactam antibiotic to the periplasm where they could bind to the penicillin binding proteins to prevent peptidoglycan crosslinking [96]. Additional insight into the mechanism of unique sensitivity to the β-lactam antibiotic in the anti- IHF NRel population was provided by the increased abundance of the peptidoglycan synthesis protein MurB, which suggested that the anti- IHF NRel were actively synthesizing peptidoglycan which would support

their greater susceptibility to the action of a β-lactam antibiotic [96,97]. The upregulation of *acrR*, which represses expression of AcrAB efflux pump, likely results in increased AMC concentration within the anti-IHF NRel and enhanced killing. The upregulation of *fis* in the anti-IHF NRel population presents yet another possible mechanism for increased sensitivity to AMC, since both *P. aeruginosa* and *E. coli* mutants with a nonfunctional *fis* gene showed enhanced resistance to a β-lactam antibiotic [98–100]. In addition to the possible mechanisms discussed above, many other factors, such as accessibility to the bacteria released from the biofilm matrix into the surrounding milieu, combined with overall changes in metabolic activity and/or alterations in membrane content and permeability could all have likely contributed to the observed susceptibilities to the specific class of antibiotic shown, as well as perhaps additional classes of antibiotics not yet tested. This premise is currently under investigation as we continue to further define the phenotypes of anti-rsPilA and anti-IHF NRel NTHI.

Taken together, our data suggested that the NRel phenotype is not 'generic,' but rather highly distinct and dependent on the antibody-mediated mechanism of release of NTHI from biofilm residence. Given that we've already shown that NRel NTHI are rapidly eradicated *in vivo* by either immune effectors alone [33,49] or when needed, in combination with co-delivered antibiotics (but now at a reduced dose) [32], it is clear that while there are phenotypic distinctions, NRel NTHI and other NRel bacterial species [29,48,54–56], appear to be in a highly vulnerable state wherein they can be much more effectively eliminated. Further investigation to characterize the likely manifold distinctions between NRel NTHI populations will include examination of environmental conditions under which biofilms are formed, maturation status and character of biofilms formed by diverse strains of NTHI as well as other genera of bacteria. Furthermore, since the two NRel populations described here represent an adaptive state, the NRel phenotype is likely dynamic over time. Indeed, dissecting the contribution of release kinetics and means to disperse or disrupt biofilms will be a focus of future investigations to fully characterize the onset and duration of the distinct antibiotic-sensitive phenotypes.

In a world 'running out of antibiotics' [101] there is a push to identify new antimicrobials, institute antibiotic stewardship and educate the public as to the dangers of inappropriate antibiotic use [102]. This situation has inspired many to attack this problem in novel and creative ways. In a Nature commentary, Rappuoli, Bloom and Black [103] suggested we combine the power of vaccine-induced antibodies with a more appropriate use of antibiotics as our "last hope against multi-drug resistant bacteria and persistent disease". Whereas their focus was on antibodies that reduce carriage, and thus transmission of antibiotic-resistant bacteria [103], we envision use of specifically induced antibodies to release biofilm-resident NTHI from these highly resistant communities so they can be killed by host immune effectors and when necessary, traditional antibiotics, with the latter now used at a markedly reduced dose and for a shorter course due to the highly sensitive phenotype of NRel NTHI. An additional potential benefit of a less frequent antibiotic treatment regimen is reduction of off-target side effects and other undesirable sequelae of oral antibiotic use; which includes development of antibiotic resistance [84,104] and/or disruption of the gut microbiome [16,105–108].

Herein, we provide proof-of-principal for this strategy to treat biofilm-associated diseases caused by NTHI via use of NRel-inducing antibodies directed against unique biofilm associated targets of this important human pathogen. Moreover, use of the species independent anti-DNABII approach broadens the potential use of this combination strategy for treatment of many other diseases caused by diverse human pathogens wherein a biofilm similarly contributes significantly to pathogenesis, chronicity, recurrence and recalcitrance to treatment. Recent humanization and demonstrated efficacy of NRel-inducing monoclonal antibodies directed against a DNABII protein both *in vitro* and *in vivo* is expected to expedite transition to human clinical trials [109,110].

CRediT authorship contribution statement

Elaine M. Mokrzan: Investigation, Methodology, Visualization, Formal analysis, Writing - review & editing. **Christian P. Ahearn:** Investigation, Methodology, Visualization, Formal analysis, Writing - review & editing. **John R. Buzzo:** Investigation, Methodology, Formal analysis, Writing - review & editing. **Laura A. Novotny:** Visualization, Formal analysis, Writing - review & editing. **Yan Zhang:** Formal analysis, Software, Writing - review & editing. **Steven D. Goodman:** Conceptualization, Formal analysis, Writing - review & editing, Supervision. **Lauren O. Bakaletz:** Conceptualization, Resources, Formal analysis, Writing - original draft, preparation, Writing - review & editing, Supervision.

Declaration of competing interest

The authors declare the following financial interests/personal relationships which may be considered as potential competing interests: L.O.B. and S.D.G. are the inventors of technology related to the DNABII proteins, rights to which have been licensed to Claremetyx Biosciences, Inc. L.O.B. is an inventor of technology related to PilA-derived immunogens that is licensed to GlaxoSmithKline Biologicals. E.M.M., C.P.A., J.R.B., L.A.N., and Y.Z. have no interests to declare.

Acknowledgements

The authors are grateful to Aishwarya Devaraj, Ph.D. for thoughtful discussions. The authors thank Joseph Jurcisek for critical manuscript review and Jennifer Neelans for outstanding assistance with manuscript preparation.

Appendix A. Supplementary data

Supplementary data to this article can be found online at https://doi.org/10.1016/j.bioflm.2020.100039.

Funding sources

This work was supported by the National Institutes of Health [NIH/NIDCD R01 DC003915 to LOB and NIH/NIDCD R01 DC011818 to LOB & SDG] as well as discretionary funds to LOB. YZ was partially supported by The Ohio State University Comprehensive Cancer Center [#P30CA016058].

References

[1] Dongari-Bagtzoglou A. Pathogenesis of mucosal biofilm infections: challenges and progress. Expert Rev Anti Infect Ther 2008;6:201–8. https://doi.org/10.1586/14787210.6.2.201.

[2] Costerton JW, Stewart PS, Greenberg EP. Bacterial biofilms: a common cause of persistent infections. Science 1999;284:1318–22. https://doi.org/10.1126/science.284.5418.1318.

[3] Flemming HC, Wingender J. The biofilm matrix. Nat Rev Microbiol 2010;8:623–33. https://doi.org/10.1038/nrmicro2415.

[4] Ahearn CP, Gallo MC, Murphy TF. Insights on persistent airway infection by nontypeable *Haemophilus influenzae* in chronic obstructive pulmonary disease. Pathog Dis 2017;75. https://doi.org/10.1093/femspd/ftx042.

[5] Cardines R, Giufre M, Pompilio A, Fiscarelli E, Ricciotti G, Di Bonaventura G, Cerquetti M. *Haemophilus influenzae* in children with cystic fibrosis: antimicrobial susceptibility, molecular epidemiology, distribution of adhesins and biofilm formation. Int J Med Microbiol 2012;302:45–52. https://doi.org/10.1016/j.ijmm.2011.08.003.

[6] Pang B, Hong W, Kock ND, Swords WE. Dps promotes survival of nontypeable *Haemophilus influenzae* in biofilm communities *in vitro* and resistance to clearance *in vivo*. Front Cell Infect Microbiol 2012;2:58. https://doi.org/10.3389/fcimb.2012.00058.

[7] Barkai G, Leibovitz E, Givon-Lavi N, Dagan R. Potential contribution by nontypable *Haemophilus influenzae* in protracted and recurrent acute otitis media. Pediatr Infect Dis J 2009;28:466–71. https://doi.org/10.1097/inf.0b013e3181950c74.

[8] Cleary D, Devine V, Morris D, Osman K, Gladstone R, Bentley S, Faust S, Clarke S. Pneumococcal vaccine impacts on the population genomics of non-typeable

Haemophilus influenzae. Microb Genom 2018;4:e000209. https://doi.org/10.1099/mgen.0.000209.
[9] Grevers G, Wiedemann S, Bohn JC, Blasius RW, Harder T, Kroeniger W, Vetter V, Pircon JY, Marano C. Identification and characterization of the bacterial etiology of clinically problematic acute otitis media after tympanocentesis or spontaneous otorrhea in German children. BMC Infect Dis 2012;12:312. https://doi.org/10.1186/1471-2334-12-312.
[10] Vergison A. Microbiology of otitis media: a moving target. Vaccine 2008;26(Suppl 7):G5–10. https://doi.org/10.1016/j.vaccine.2008.11.006.
[11] Wiertsema SP, Kirkham LA, Corscadden KJ, Mowe EN, Bowman JM, Jacoby P, Francis R, Vijayasekaran S, Coates HL, Riley TV, Richmond P. Predominance of nontypeable *Haemophilus influenzae* in children with otitis media following introduction of a 3+0 pneumococcal conjugate vaccine schedule. Vaccine 2011; 29:5163–70. https://doi.org/10.1016/j.vaccine.2011.05.035.
[12] Hassan F. Molecular mechanisms of *Moraxella catarrhalis*-induced otitis media. Curr Allergy Asthma Rep 2013;13:512–7. https://doi.org/10.1007/s11882-013-0374-8.
[13] Mittal R, Parrish JM, Soni M, Mittal J, Mathee K. Microbial otitis media: recent advancements in treatment, current challenges and opportunities. J Med Microbiol 2018;67:1417–25. https://doi.org/10.1099/jmm.0.000810.
[14] Belfield K, Bayston R, Birchall JP, Daniel M. Do orally administered antibiotics reach concentrations in the middle ear sufficient to eradicate planktonic and biofilm bacteria? A review. Int J Pediatr Otorhinolaryngol 2015;79:296–300. https://doi.org/10.1016/j.ijporl.2015.01.003.
[15] Gilbert JA, Blaser MJ, Caporaso JG, Jansson JK, Lynch SV, Knight R. Current understanding of the human microbiome. Nat Med 2018;24:392–400. https://doi.org/10.1038/nm.4517.
[16] Kuehn J, Ismael Z, Long PF, Barker CI, Sharland M. Reported rates of diarrhea following oral penicillin therapy in pediatric clinical trials. J Pediatr Pharmacol Therapeut 2015;20:90–104. https://doi.org/10.5863/1551-6776-20.2.90.
[17] Lamont RF, Moller Luef B, Stener Jorgensen J. Childhood inflammatory and metabolic disease following exposure to antibiotics in pregnancy. antenatally, intrapartum and neonatally 2020;F1000Res 9:F1000. https://doi.org/10.12688/f1000research.19954.1. Faculty Rev-1144.
[18] Beekmann SE, Heilmann KP, Richter SS, Garcia-de-Lomas J, Doern GV, Group GS. Antimicrobial resistance in *Streptococcus pneumoniae, Haemophilus influenzae, Moraxella catarrhalis* and group A beta-haemolytic streptococci in 2002-2003. Results of the multinational GRASP Surveillance Program. Int J Antimicrob Agents 2005;25:148–56. https://doi.org/10.1016/j.ijantimicag.2004.09.016.
[19] Leibovitz E, Broides A, Greenberg D, Newman N. Current management of pediatric acute otitis media. Expert Rev Anti Infect Ther 2010;8:151–61. https://doi.org/10.1586/eri.09.112.
[20] Song JH, Dagan R, Klugman KP, Fritzell B. The relationship between pneumococcal serotypes and antibiotic resistance. Vaccine 2012;30:2728–37. https://doi.org/10.1016/j.vaccine.2012.01.091.
[21] Andre FE, Booy R, Bock HL, Clemens J, Datta SK, John TJ, Lee BW, Lolekha S, Peltola H, Ruff TA, Santosham M, Schmitt HJ. Vaccination greatly reduces disease, disability, death and inequity worldwide. Bull World Health Organ 2008;86: 140–6. https://doi.org/10.2471/blt.07.040089.
[22] Bakaletz LO, Baker BD, Jurcisek JA, Harrison A, Novotny LA, Bookwalter JE, Mungur R, Munson Jr RS. Demonstration of type IV pilus expression and a twitching phenotype by *Haemophilus influenzae*. Infect Immun 2005;73:1635–43. https://doi.org/10.1128/IAI.73.3.1635-1643.2005.
[23] Carruthers MD, Tracy EN, Dickson AC, Ganser KB, Munson Jr RS, Bakaletz LO. Biological roles of nontypeable *Haemophilus influenzae* type IV pilus proteins encoded by the pil and com operons. J Bacteriol 2012;194:1927–33. https://doi.org/10.1128/JB.06540-11.
[24] Das J, Mokrzan E, Lakhani V, Rosas L, Jurcisek JA, Ray WC, Bakaletz LO. Extracellular DNA and type IV pilus expression regulate the structure and kinetics of biofilm formation by nontypeable *Haemophilus influenzae*. mBio 2017;8. https://doi.org/10.1128/mBio.01466-17. e01466-01417.
[25] Jurcisek JA, Bookwalter JE, Baker BD, Fernandez S, Novotny LA, Munson Jr RS, Bakaletz LO. The PilA protein of non-typeable *Haemophilus influenzae* plays a role in biofilm formation, adherence to epithelial cells and colonization of the mammalian upper respiratory tract. Mol Microbiol 2007;65:1288–99. https://doi.org/10.1111/j.1365-2958.2007.05864.x.
[26] Mokrzan EM, Johnson TJ, Bakaletz LO. Expression of the nontypeable *Haemophilus influenzae* type IV pilus is stimulated by coculture with host respiratory tract epithelial cells. Infect Immun 2019;87. https://doi.org/10.1128/IAI.00704-19. e00704-00719.
[27] Mokrzan EM, Ward MO, Bakaletz LO. Type IV pilus expression is upregulated in nontypeable *Haemophilus influenzae* biofilms formed at the temperature of the human nasopharynx. J Bacteriol 2016;198:2619–30. https://doi.org/10.1128/JB.01022-15.
[28] Toone SL, Ratkiewicz M, Novotny LA, Phong BL, Bakaletz LO. Nontypeable *Haemophilus influenzae* Type IV pilus mediates augmented adherence to rhinovirus-infected human airway epithelial cells. Infect Immun 2020. https://doi.org/10.1128/IAI.00248-20.
[29] Mokrzan EM, Novotny LA, Brockman KL, Bakaletz LO. Antibodies against the majority subunit (PilA) of the type IV pilus of nontypeable *Haemophilus influenzae* disperse *Moraxella catarrhalis* from a dual-species biofilm. mBio 2018;9. https://doi.org/10.1128/mBio.02423-18. e02423-02418.
[30] Novotny LA, Adams LD, Kang DR, Wiet GJ, Cai X, Sethi S, Murphy TF, Bakaletz LO. Epitope mapping immunodominant regions of the PilA protein of nontypeable *Haemophilus influenzae* (NTHI) to facilitate the design of two novel chimeric vaccine candidates. Vaccine 2009;28:279–89. https://doi.org/10.1016/j.vaccine.2009.08.017.
[31] Novotny LA, Clements JD, Bakaletz LO. Kinetic analysis and evaluation of the mechanisms involved in the resolution of experimental nontypeable *Haemophilus influenzae*-induced otitis media after transcutaneous immunization. Vaccine 2013b;31:3417–26. https://doi.org/10.1016/j.vaccine.2012.10.033.
[32] Novotny LA, Jurcisek JA, Goodman SD, Bakaletz LO. Monoclonal antibodies against DNA-binding tips of DNABII proteins disrupt biofilms *in vitro* and induce bacterial clearance *in vivo*. EBioMedicine 2016;10:33–44. https://doi.org/10.1016/j.ebiom.2016.06.022.
[33] Novotny LA, Jurcisek JA, Ward Jr MO, Jordan ZB, Goodman SD, Bakaletz LO. Antibodies against the majority subunit of type IV Pili disperse nontypeable *Haemophilus influenzae* biofilms in a LuxS-dependent manner and confer therapeutic resolution of experimental otitis media. Mol Microbiol 2015;96: 276–92. https://doi.org/10.1111/mmi.12934.
[34] Ysebaert C, Denoel P, Weynants V, Bakaletz LO, Novotny LA, Godfroid F, Hermand P. A protein E-PilA fusion protein shows vaccine potential against nontypeable *Haemophilus influenzae* in mice and chinchillas. Infect Immun 2019; 87. https://doi.org/10.1128/IAI.00345-19. e00345-00319.
[35] Armbruster CE, Hong W, Pang B, Dew KE, Juneau RA, Byrd MS, Love CF, Kock ND, Swords WE. LuxS promotes biofilm maturation and persistence of nontypeable *Haemophilus influenzae in vivo* via modulation of lipooligosaccharides on the bacterial surface. Infect Immun 2009;77:4081–91. https://doi.org/10.1128/IAI.00320-09.
[36] Daines DA, Bothwell M, Furrer J, Unrath W, Nelson K, Jarisch J, Melrose N, Greiner L, Apicella M, Smith AL. *Haemophilus influenzae* luxS mutants form a biofilm and have increased virulence. Microb Pathog 2005;39:87–96. https://doi.org/10.1016/j.micpath.2005.06.003.
[37] Surette MG, Miller MB, Bassler BL. Quorum sensing in *Escherichia coli, Salmonella typhimurium*, and *Vibrio harveyi*: a new family of genes responsible for autoinducer production. Proc Natl Acad Sci U S A 1999;96:1639–44. https://doi.org/10.1073/pnas.96.4.1639.
[38] Armbruster CE, Pang B, Murrah K, Juneau RA, Perez AC, Weimer KE, Swords WE. RbsB (NTHI_0632) mediates quorum signal uptake in nontypeable *Haemophilus influenzae* strain 86-028NP. Mol Microbiol 2011;82:836–50. https://doi.org/10.1111/j.1365-2958.2011.07831.x.
[39] Pang B, Armbruster CE, Foster G, Learman BS, Gandhi U, Swords WE. Autoinducer 2 (AI-2) production by nontypeable *Haemophilus influenzae* 86-028NP promotes expression of a predicted glycosyltransferase that is a determinant of biofilm maturation, prevention of dispersal, and persistence *in vivo*. Infect Immun 2018; 86. https://doi.org/10.1128/IAI.00506-18.
[40] Armbruster CE, Hong W, Pang B, Weimer KE, Juneau RA, Turner J, Swords WE. Indirect pathogenicity of *Haemophilus influenzae* and *Moraxella catarrhalis* in polymicrobial otitis media occurs via interspecies quorum signaling. mBio 2010;1. https://doi.org/10.1128/mBio.00102-10. e00102- 00110.
[41] Kamashev D, Agapova Y, Rastorguev S, Talyzina AA, Boyko KM, Korzhenevskiy DA, Vlaskina A, Vasilov R, Timofeev VI, Rakitina TV. Comparison of histone-like HU protein DNA-binding properties and HU/IHF protein sequence alignment. PloS One 2017;12:e0188037. https://doi.org/10.1371/journal.pone.0188037.
[42] Devaraj A, Buzzo J, Rocco CJ, Bakaletz LO, Goodman SD. The DNABII family of proteins is comprised of the only nucleoid associated proteins required for nontypeable *Haemophilus influenzae* biofilm structure. Microbiol 2018;7:e00563. https://doi.org/10.1002/mbo3.563.
[43] Devaraj A, Justice SS, Bakaletz LO, Goodman SD. DNABII proteins play a central role in UPEC biofilm structure. Mol Microbiol 2015;96:1119–35. https://doi.org/10.1111/mmi.12994.
[44] Novotny LA, Amer AO, Brockson ME, Goodman SD, Bakaletz LO. Structural stability of *Burkholderia cenocepacia* biofilms is reliant on eDNA structure and presence of a bacterial nucleic acid binding protein. PloS One 2013a;8:e67629. https://doi.org/10.1371/journal.pone.0067629.
[45] Goodman SD, Obergfell KP, Jurcisek JA, Novotny LA, Downey JS, Ayala EA, Tjokro N, Li B, Justice SS, Bakaletz LO. Biofilms can be dispersed by focusing the immune system on a common family of bacterial nucleoid-associated proteins. Mucosal Immunol 2011;4:625–37. https://doi.org/10.1038/mi.2011.27.
[46] Jurcisek JA, Bakaletz LO. Biofilms formed by nontypeable *Haemophilus influenzae in vivo* contain both double-stranded DNA and type IV pilin protein. J Bacteriol 2007;189:3868–75. https://doi.org/10.1128/JB.01935-06.
[47] Whitchurch CB, Tolker-Nielsen T, Ragas PC, Mattick JS. Extracellular DNA required for bacterial biofilm formation. Science 2002;295:1487. https://doi.org/10.1126/science.295.5559.1487.
[48] Brockson ME, Novotny LA, Mokrzan EM, Malhotra S, Jurcisek JA, Akbar R, Devaraj A, Goodman SD, Bakaletz LO. Evaluation of the kinetics and mechanism of action of anti-integration host factor-mediated disruption of bacterial biofilms. Mol Microbiol 2014;93:1246–58. https://doi.org/10.1111/mmi.12735.
[49] Novotny LA, Goodman SD, Bakaletz LO. Redirecting the immune response towards immunoprotective domains of a DNABII protein resolves experimental otitis media. NPJ Vaccines 2019;4:43. https://doi.org/10.1038/s41541-019-0137-1.
[50] Freire MO, Devaraj A, Young A, Navarro JB, Downey JS, Chen C, Bakaletz LO, Zadeh HH, Goodman SD. A bacterial-biofilm-induced oral osteolytic infection can be successfully treated by immuno-targeting an extracellular nucleoid-associated protein. Mol Oral Microbiol 2017;32:74–88. https://doi.org/10.1111/omi.12155.
[51] Chua SL, Liu Y, Yam JK, Chen Y, Vejborg RM, Tan BG, Kjelleberg S, Tolker-Nielsen T, Givskov M, Yang L. Dispersed cells represent a distinct stage in the

transition from bacterial biofilm to planktonic lifestyles. Nat Commun 2014;5:4462. https://doi.org/10.1038/ncomms5462.
[52] Marks LR, Davidson BA, Knight PR, Hakansson AP. Interkingdom signaling induces *Streptococcus pneumoniae* biofilm dispersion and transition from asymptomatic colonization to disease. mBio 2013;4. https://doi.org/10.1128/mBio.00438-13. e00438-00413.
[53] Sauer K, Cullen MC, Rickard AH, Zeef LA, Davies DG, Gilbert P. Characterization of nutrient-induced dispersion in *Pseudomonas aeruginosa* PAO1 biofilm. J Bacteriol 2004;186:7312–26. https://doi.org/10.1128/JB.186.21.7312-7326.2004.
[54] Chambers JR, Cherny KE, Sauer K. Susceptibility of *Pseudomonas aeruginosa* dispersed cells to antimicrobial agents is dependent on the dispersion cue and class of the antimicrobial agent used. Antimicrob Agents Chemother 2017;61. https://doi.org/10.1128/AAC.00846-17. e00846-00817.
[55] Goodwine J, Gil J, Doiron A, Valdes J, Solis M, Higa A, Davis S, Sauer K. Pyruvate-depleting conditions induce biofilm dispersion and enhance the efficacy of antibiotics in killing biofilms *in vitro* and *in vivo*. Sci Rep 2019;9:3763. https://doi.org/10.1038/s41598-019-40378-z.
[56] Petrova OE, Sauer K. Escaping the biofilm in more than one way: desorption, detachment or dispersion. Curr Opin Microbiol 2016;30:67–78. https://doi.org/10.1016/j.mib.2016.01.004.
[57] Harrison A, Dyer DW, Gillaspy A, Ray WC, Mungur R, Carson MB, Zhong H, Gipson J, Gipson M, Johnson LS, Lewis L, Bakaletz LO, Munson Jr RS. Genomic sequence of an otitis media isolate of nontypeable *Haemophilus influenzae*: comparative study with *H. influenzae* serotype d, strain KW20. J Bacteriol 2005;187:4627–36. https://doi.org/10.1128/JB.187.13.4627-4636.2005.
[58] Sirakova T, Kolattukudy PE, Murwin D, Billy J, Leake E, Lim D, DeMaria T, Bakaletz L. Role of fimbriae expressed by nontypeable *Haemophilus influenzae* in pathogenesis of and protection against otitis media and relatedness of the fimbrin subunit to outer membrane protein A. Infect Immun 1994;62:2002–20.
[59] Jurcisek JA, Dickson AC, Bruggeman ME, Bakaletz LO. *In vitro* biofilm formation in an 8-well chamber slide. JoVE 2011;20:2481. https://doi.org/10.3791/2481.
[60] Lê S, Josse J, Husson F. FactoMineR: a package for multivariate analysis. J Stat Software 2008;25:1–18. https://doi.org/10.18637/jss.v025.i01.
[61] Wickham H, Chang W, Henry L, Pedersen TL, Takahashi K, Wilke C, Woo K, Yutani H, Dunnington D. ggplot2: elegant graphics for data analysis. New York: Springer-Verlag; 2016.
[62] Aziz A, Sarovich DS, Nosworthy E, Beissbarth J, Chang AB, Smith-Vaughan H, Price EP, Harris TM. Molecular signatures of non-typeable *Haemophilus influenzae* lung adaptation in pediatric chronic lung disease. Front Microbiol 2019;10:1622. https://doi.org/10.3389/fmicb.2019.01622.
[63] Tatusov RL, Galperin MY, Natale DA, Koonin EV. The COG database: a tool for genome-scale analysis of protein functions and evolution. Nucleic Acids Res 2000;28:33–6. https://doi.org/10.1093/nar/28.1.33.
[64] Poole J, Foster E, Chaloner K, Hunt J, Jennings MP, Bair T, Knudtson K, Christensen E, Munson Jr RS, Winokur PL, Apicella MA. Analysis of nontypeable *Haemophilus influenzae* phase-variable genes during experimental human nasopharyngeal colonization. J Infect Dis 2013;208:720–7. https://doi.org/10.1093/infdis/jit240.
[65] Swords WE, Jones PA, Apicella MA. The lipo-oligosaccharides of *Haemophilus influenzae*: an interesting array of characters. J Endotoxin Res 2003;9:131–44. https://doi.org/10.1179/096805103125001531.
[66] Kaplan E, Greene NP, Crow A, Koronakis V. Insights into bacterial lipoprotein trafficking from a structure of LolA bound to the LolC periplasmic domain. Proc Natl Acad Sci U S A 2018;115:E7389–97. https://doi.org/10.1073/pnas.1806822115.
[67] Parsons JB, Rock CO. Bacterial lipids: metabolism and membrane homeostasis. Prog Lipid Res 2013;52:249–76. https://doi.org/10.1016/j.plipres.2013.02.002.
[68] Murphy TF, Kirkham C, Lesse AJ. Construction of a mutant and characterization of the role of the vaccine antigen P6 in outer membrane integrity of nontypeable *Haemophilus influenzae*. Infect Immun 2006;74:5169–76. https://doi.org/10.1128/IAI.00692-06.
[69] Sikkema DJ, Murphy TF. Molecular analysis of the P2 porin protein of nontypeable *Haemophilus influenzae*. Infect Immun 1992;60:5204–11. https://doi.org/10.1128/IAI.60.12.5204-5211.1992.
[70] Rolfe MD, Rice CJ, Lucchini S, Pin C, Thompson A, Cameron AD, Alston M, Stringer MF, Betts RP, Baranyi J, Peck MW, Hinton JC. Lag phase is a distinct growth phase that prepares bacteria for exponential growth and involves transient metal accumulation. J Bacteriol 2012;194:686–701. https://doi.org/10.1128/JB.06112-11.
[71] Nikolaidis I, Favini-Stabile S, Dessen A. Resistance to antibiotics targeted to the bacterial cell wall. Protein Sci 2014;23:243–59. https://doi.org/10.1002/pro.2414.
[72] Harrison CJ, Woods C, Stout G, Martin B, Selvarangan R. Susceptibilities of *Haemophilus influenzae, Streptococcus pneumoniae*, including serotype 19A, and Moraxella catarrhalis paediatric isolates from 2005 to 2007 to commonly used antibiotics. J Antimicrob Chemother 2009;63:511–9. https://doi.org/10.1093/jac/dkn538.
[73] K LCH, Akyol S, Parkan OM, Dinc G, Sav H, Aydemir G. Molecular characterization and antibiotic susceptibility of *Haemophilus influenzae* clinical isolates. Inf Med 2017;25:27–32.
[74] Pelton S. In: Post T, editor. Acute otitis media in children: Treatment. Waltham, MA: UpToDate; 2020.
[75] Sethi S, Murphy TF. Infection in the pathogenesis and course of chronic obstructive pulmonary disease. N Engl J Med 2008;359:2355–65. https://doi.org/10.1056/NEJMra0800353.
[76] Tristram S, Jacobs MR, Appelbaum PC. Antimicrobial resistance in *Haemophilus influenzae*. Clin Microbiol Rev 2007;20:368–89. https://doi.org/10.1128/CMR.00040-06.
[77] Wald ER, DeMuri GP. Antibiotic recommendations for acute otitis media and acute bacterial sinusitis: conundrum no more. Pediatr Infect Dis J 2018;37:1255–7. https://doi.org/10.1097/INF.0000000000002009.
[78] Wasserman RC, Gerber JS. Acute otitis media in the 21st century: what now? Pediatrics 2017;140. https://doi.org/10.1542/peds.2017-1966.
[79] Kapoor G, Saigal S, Elongavan A. Action and resistance mechanisms of antibiotics: a guide for clinicians. J Anaesthesiol Clin Pharmacol 2017;33:300–5. https://doi.org/10.4103/joacp.JOACP_349_15.
[80] Huovinen P. Resistance to trimethoprim-sulfamethoxazole. Clin Infect Dis 2001;32:1608–14. https://doi.org/10.1086/320532.
[81] Du D, Wang-Kan X, Neuberger A, van Veen HW, Pos KM, Piddock LJV, Luisi BF. Multidrug efflux pumps: structure, function and regulation. Nat Rev Microbiol 2018;16:523–39. https://doi.org/10.1038/s41579-018-0048-6.
[82] Barrero MA, Pietralonga PA, Schwarz DG, Silva Jr A, Paula SO, Moreira MA. Effect of the inhibitors phenylalanine arginyl ss-naphthylamide (PAssN) and 1-(1-naphthylmethyl)-piperazine (NMP) on expression of genes in multidrug efflux systems of *Escherichia coli* isolates from bovine mastitis. Res Vet Sci 2014;97:176–81. https://doi.org/10.1016/j.rvsc.2014.05.013.
[83] Anes J, McCusker MP, Fanning S, Martins M. The ins and outs of RND efflux pumps in Escherichia coli. Front Microbiol 2015;6:587. https://doi.org/10.3389/fmicb.2015.00587.
[84] Tagliabue A, Rappuoli R. Changing priorities in vaccinology: antibiotic resistance moving to the top. Front Immunol 2018;9:1068. https://doi.org/10.3389/fimmu.2018.01068.
[85] Koff WC, Schenkelberg T. The future of vaccine development. Vaccine 2019. https://doi.org/10.1016/j.vaccine.2019.07.101.
[86] 2017a Antibacterial agents in clinical development: an analysis of the antibacterial clinical development pipeline, including tuberculosis. Geneva: World Health Organization. https://apps.who.int/iris/bitstream/handle/10665/258965/WHO-EMP-IAU-2017.11-eng.pdf;jsessionid=4C4B74B963CED463A94DD2DE9CB5EACA?sequence=1.
[87] Ribeiro da Cunha B, Fonseca LP, Calado CRC. Antibiotic discovery: where have we come from, where do we go? Antibiotics 2019;8:45. https://doi.org/10.3390/antibiotics8020045.
[88] Hall CW, Mah TF. Molecular mechanisms of biofilm-based antibiotic resistance and tolerance in pathogenic bacteria. FEMS Microbiol Rev 2017;41:276–301. https://doi.org/10.1093/femsre/fux010.
[89] Sharma D, Misba L, Khan AU. Antibiotics versus biofilm: an emerging battleground in microbial communities. Antimicrob Resist Infect Contr 2019;8:76. https://doi.org/10.1186/s13756-019-0533-3.
[90] Silva MD, Sillankorva S. Otitis media pathogens - a life entrapped in biofilm communities. Crit Rev Microbiol 2019;45:595–612. https://doi.org/10.1080/1040841X.2019.1660616.
[91] Stewart PS. Mechanisms of antibiotic resistance in bacterial biofilms. Int J Med Microbiol 2002;292:107–13. https://doi.org/10.1078/1438-4221-00196.
[92] Guilhen C, Charbonnel N, Parisot N, Gueguen N, Iltis A, Forestier C, Balestrino D. Transcriptional profiling of *Klebsiella pneumoniae* defines signatures for planktonic, sessile and biofilm-dispersed cells. BMC Genom 2016;17:237. https://doi.org/10.1186/s12864-016-2557-x.
[93] Pettigrew MM, Marks LR, Kong Y, Gent JF, Roche-Hakansson H, Hakansson AP. Dynamic changes in the *Streptococcus pneumoniae* transcriptome during transition from biofilm formation to invasive disease upon influenza A virus infection. Infect Immun 2014;82:4607–19. https://doi.org/10.1128/IAI.02225-14.
[94] Rumbaugh KP, Sauer K. Biofilm dispersion. Nat Rev Microbiol 2020. https://doi.org/10.1038/s41579-020-0385-0.
[95] Fernandez-Villa D, Aguilar MR, Rojo L. Folic acid antagonists: antimicrobial and immunomodulating mechanisms and applications. Int J Mol Sci 2019;20:4996. https://doi.org/10.3390/ijms20204996.
[96] Delcour AH. Outer membrane permeability and antibiotic resistance. Biochim Biophys Acta 2009;1794:808–16. https://doi.org/10.1016/j.bbapap.2008.11.005.
[97] Zapun A, Contreras-Martel C, Vernet T. Penicillin-binding proteins and beta-lactam resistance. FEMS Microbiol Rev 2008;32:361–85. https://doi.org/10.1111/j.1574-6976.2007.00095.x.
[98] Grkovic S, Brown MH, Skurray RA. Transcriptional regulation of multidrug efflux pumps in bacteria. Semin Cell Dev Biol 2001;12:225–37. https://doi.org/10.1006/scdb.2000.0248.
[99] Long Y, Fu W, Wang S, Deng X, Jin Y, Bai F, Cheng Z, Wu W. Fis Contributes to resistance of *Pseudomonas aeruginosa* to ciprofloxacin by regulating pyocin synthesis. J Bacteriol 2020;202. https://doi.org/10.1128/JB.00064-20.
[100] Martin RG, Rosner JL. Fis, an accessorial factor for transcriptional activation of the mar (multiple antibiotic resistance) promoter of *Escherichia coli* in the presence of the activator MarA, SoxS, or Rob. J Bacteriol 1997;179:7410–9. https://doi.org/10.1128/jb.179.23.7410-7419.1997.
[101] 2017b reportThe world is running out of antibiotics, WHO report confirms. Geneva, World Health Organization. https://www.who.int/news-room/detail/20-09-2017-the-world-is-running-out-of-antibiotics-who-report-confirms.
[102] Piltcher OB, Kosugi EM, Sakano E, Mion O, Testa JRG, Romano FR, Santos MCJ, Di Francesco RC, Mitre EI, Bezerra TFP, Roithmann R, Padua FG, Valera FCP, Lubianca Neto JF, Sa LCB, Pignatari SSN, Avelino MAG, Caixeta JAS, Anselmo-Lima WT, Tamashiro E. How to avoid the inappropriate use of antibiotics in upper respiratory tract infections? A position statement from an expert panel. Braz J Otorhinolaryngol 2018;84:265–79. https://doi.org/10.1016/j.bjorl.2018.02.001.

[103] Rappuoli R, Bloom DE, Black S. Deploy vaccines to fight superbugs. Nature 2017; 552:165–7. https://doi.org/10.1038/d41586-017-08323-0.
[104] Patini R, Mangino G, Martellacci L, Quaranta G, Masucci L, Gallenzi P. The effect of different antibiotic regimens on bacterial resistance: a systematic review. Antibiotics 2020;9:22. https://doi.org/10.3390/antibiotics9010022.
[105] Bailey MT, Lauber CL, Novotny LA, Goodman SD, Bakaletz LO. Immunization with a biofilm-disrupting nontypeable *Haemophilus influenzae* vaccine antigen did not alter the gut microbiome in chinchillas, unlike oral delivery of a broad-spectrum antibiotic commonly used for otitis media. mSphere 2020;5. https://doi.org/10.1128/mSphere.00296-20. e00296-00220.
[106] Gillies M, Ranakusuma A, Hoffmann T, Thorning S, McGuire T, Glasziou P, Del Mar C. Common harms from amoxicillin: a systematic review and meta-analysis of randomized placebo-controlled trials for any indication. CMAJ (Can Med Assoc J) 2015;187:E21–31. https://doi.org/10.1503/cmaj.140848.
[107] MacPherson CW, Mathieu O, Tremblay J, Champagne J, Nantel A, Girard SA, Tompkins TA. Gut bacterial microbiota and its resistome rapidly recover to basal state levels after short-term amoxicillin-clavulanic acid treatment in healthy adults. Sci Rep 2018;8:11192. https://doi.org/10.1038/s41598-018-29229-5.
[108] Pallav K, Dowd SE, Villafuerte J, Yang X, Kabbani T, Hansen J, Dennis M, Leffler DA, Newburg DS, Kelly CP. Effects of polysaccharopeptide from Trametes versicolor and amoxicillin on the gut microbiome of healthy volunteers: a randomized clinical trial. Gut Microb 2014;5:458–67. https://doi.org/10.4161/gmic.29558.
[109] D'Andrea MM, Lau GW. DNABII targeting antibodies as vaccines against biofilm diseases. EBioMedicine 2020;58:102921. https://doi.org/10.1016/j.ebiom.2020.102921.
[110] Novotny LA, Goodman SD, Bakaletz LO. Targeting a bacterial DNABII protein with a chimeric peptide immunogen or humanised monoclonal antibody to prevent or treat recalcitrant biofilm-mediated infections. EBioMedicine 2020. https://doi.org/10.1016/j.ebiom.2020.102867.